Transition entropy, Helmholtz free energy, and heat capacity of free-standing smectic films above the bulk smectic-*A*—isotropic transition temperature: A mean-field treatment

A. V. Zakharov*
Saint Petersburg Institute for Machine Sciences, The Russian Academy of Sciences, Saint Petersburg 199178, Russia

D. E. Sullivan†
Department of Physics and Guelph-Waterloo Physics Institute, University of Guelph, Guelph, Ontario, Canada N1G 2W1

(Received 24 November 2009; revised manuscript received 2 July 2010; published 13 October 2010)

We have carried out a numerical study of both the structural and thermodynamic properties of free-standing smectic films (FSSFs) for two cases of enhanced pair interactions in the bounding layers. Calculations, based upon the extended McMillan's approach with anisotropic forces, shows a stepwise reduction of the value of the heat capacity as the temperature is raised above the bulk smectic A-isotropic transition. The effects of surface "enhanced" pair interactions in the bounding layers and of film thickness on the orientational and translational order parameters, the Helmholtz free energy, and entropy of FSSFs have also been investigated. Reasonable agreement between the theoretically predicted and the experimentally obtained—by means of calorimetric techniques—data on the heat capacity of the partially fluorinated5-*n*-alkyl-2-(4-*n*-(perfluoroalkyl-metheleneoxy)phenyl) (H10F5MOPP) films has been obtained.

DOI: 10.1103/PhysRevE.82.041704 PACS number(s): 61.30.Hn

I. INTRODUCTION

One of the most interesting features of many smectic liquid crystals (LCs) is that, under appropriate conditions, they can be spread across an opening to form free-standing smectic films (FSSFs) [1]. In this work, we are concerned with FSSFs having a layered smectic-A (SmA) structure, in which the long axes of molecules are normal to the planes containing the layers and the intermolecular spacing is roughly the length of the molecule. Because the smectic layer normal is parallel to the film normal, the FSSF thickness is quantized in units of layers. Even films only 2 molecular layers thick can be readily prepared. The surface tension at the film-vapor interface acts to promote smectic order at the surface resulting in the surface layers ordering at a higher temperature than the interior [2,3]. It is generally expected that rough interfaces cause the surface region to grow continuously upon approaching the bulk transition temperature, whereas smooth interfaces favor layer-by-layer growth [2]. In such quasi-two-dimensional systems the melting originates in the interior of the film and penetrates toward the surface. The study of these films is therefore important to our understanding of the impact of reduced dimensionality and the importance of surface effects.

A great variety of phenomena can be observed in thin FSSFs; interlayer structure [3], wetting [4,5], surface transition [6–8] phenomena and heat-capacity anomalies [2,9]. For instance, the wetting phenomenon is a prominent example where the surface anchoring potential plays an important role in the layering and rupturing processes [5,10]. In particular, it was predicted that an enhancement of the surface anchoring can drive a crossover from partial to complete wetting at the SmA-isotropic (*AI*) transition temperature T_{AI} [10].

Another interesting phenomenon in certain free-standing smectic films is the occurrence of layer-thinning transitions [2,11–14]. Both by calorimetric and optical studies on free-standing partially fluorinated LC films, it has been shown that the SmA-I transition occurs through a series of layer-thinning transitions, causing the films to thin in a stepwise manner as the temperature is increased above the bulk SmA-I transition temperature [2]. These transitions have been attributed to the reduction of smectic fluctuations in the boundary layers. Associated phenomena have been observed in the heat capacities near the layer-thinning transition temperatures. These have been studied in different compounds [2,9] and consist of stepwise reductions of the value of $C_p(T)$ as the temperature T is raised above that of the bulk transition temperature. The calorimetric studies have shown that the reduction of $C_p(T)$ is associated with the reduction of the number of layers in the film, but at the current moment there is no theoretical description of this effect as the temperature is raised above the bulk smectic A-isotropic transition temperature. This is the main objective of the present article.

II. MODEL AND CALCULATIONS

In this work, we investigate the structural and thermodynamic properties, such as the Helmholtz free energy, entropy, and heat capacity, of FSSFs composed of smectic-A layers. This will be done in the framework of the extended McMillan's mean-field approach with anisotropic forces [15]. Our form of this theory for free-standing smectic films differs from that first introduced by Mirantsev [14]. The latter is based on introducing a surface parameter W_0 representing the strength of an "external" homeotropic surface anchoring field, which we feel is more appropriate for a film bounded by solid substrates. In the present work, we replace the external anchoring field by "enhanced" pair interactions in the bounding layers, as discussed in [16,17].

*Author to whom correspondence should be addressed; avz0911@yahoo.com; www.ipme.ru
†sullivan@uoguelph.ca; www.physics.uoguelph.ca

With that in mind, a free-standing smectic-A film composed of N discrete smectic layers with a thickness of the order of the molecular length d and with total number of particles $M=\Sigma_{i=1}^{N}N_i$ will be considered. Here the number of molecules per layer N_i is assumed to be the same for all layers. The molecules within each layer are assumed to interact only with molecules of the same layer and those of the two neighboring ones. In the framework of that approach, the effective anisotropic potentials $\Phi_i(i=1,\ldots,N)$ within the ith smectic layer can be introduced [14,15]

$$\Phi_1(z_1,\theta_1)=-\frac{V_0}{3}\left[\frac{W_0}{V_0}q_1+q_2+\alpha\cos\left(\frac{2\pi z_1}{d}\right)\times\left(\frac{W_0}{V_0}\sigma_1+\sigma_2\right)\right]P_2(\cos\,\theta_1),$$

$$\Phi_{1<i<N}(z_i,\theta_i)=-\frac{V_0}{3}\left[\sum_{j=i-1}^{i+1}q_j+\alpha\cos\left(\frac{2\pi z_i}{d}\right)\sum_{j=i-1}^{i+1}\sigma_j\right]\times P_2(\cos\,\theta_i),$$

$$\Phi_N(z_N,\theta_N)=-\frac{V_0}{3}\left[\frac{W_0}{V_0}q_N+q_{N-1}+\alpha\cos\left(\frac{2\pi z_N}{d}\right)\left(\frac{W_0}{V_0}\sigma_N+\sigma_{N-1}\right)\right]P_2(\cos\,\theta_N),\tag{1}$$

where z_i is the distance along the z-axis normal to the ith smectic plane, θ_i is the polar angle between the long axis of the molecule belonging to the ith layer and the z direction, $P_2(\cos\,\theta_i)$ is the second-order Legendre polynomial, V_0 is the parameter of the system which determines the scale of the nematic-isotropic transition temperature and fixes the temperature scale of the model, W_0 is the parameter corresponding to "enhanced" pair interactions in the bounding layers, and $\alpha=2\exp[-(\frac{\pi r_0}{d})^2]$ is the one extra parameter of the system which can be varied between 0 and 2, and reflects the length of the *alkyl* tails of calamatic molecules [15]. Here r_0 is a characteristic length associated with the rigid core of the molecule. Physically, this model indicates that we replace V_0 by W_0 within the first and last layers, whereas for all interior layers $1<i<N$ the interaction coefficient V_0 has not changed. Both orientational q_i and translational σ_i order parameters (OPs) for the ith layer satisfy the self-consistent nonlinear equations

$$q_i=\langle P_2(\cos\,\theta_i)\rangle_i,\tag{2}$$

and

$$\sigma_i=\left\langle\cos\left(\frac{2\pi z_i}{d}\right)P_2(\cos\,\theta_i)\right\rangle_i,\tag{3}$$

where $\langle(\ldots)\rangle_i$ is the statistical-mechanical average with respect to the one-particle distribution function of the ith layer

$$h_i(z_i,\theta_i)=\mathcal{A}_i^{-1}\exp\left[-\frac{\Phi_i}{k_BT}\right],\tag{4}$$

where $\mathcal{A}_i$ is a normalization constant, and T is the absolute temperature of the system.

As mentioned earlier, this form of the extension of McMillan's approach for describing the structural and thermodynamic of free-standing smectic films differs from that introduced by Mirantsev [14]. In the latter case, for the first bounding layer ($i=1$), the expression for the effective anisotropic potential $\Phi_1(z_1,\theta_1)$ was written as [14] $\Phi_1(z_1,\theta_1)=-\frac{V_0}{3}[q_1+q_2+\frac{3W_0}{V_0}+\alpha\cos(\frac{2\pi z_1}{d})(\sigma_1+\sigma_2)]P_2(\cos\,\theta_1)$, and similarly for $\Phi_N(z_N,\theta_N)$. In the present case the role of "surface enhancement" is played by the additional pair interaction $\frac{W_0-V_0}{3}[q_{1(N)}+\alpha\cos(\frac{2\pi z_1}{d})\sigma_{1(N)}]$, which couples to both OPs $q_{1(N)}$ and $\sigma_{1(N)}$ by symmetry with all interior layers. As a result, these two approaches give different expressions not only for the Helmholtz free energy f, but also for the entropy s and heat capacity c_v.

The set of OPs q_i and σ_i corresponding to the ith layer of the smectic film composed of a stack of N smectic-A layers can be obtained by solving the system of $2N$ nonlinear self-consistent Eqs. (2)–(4), at a given number of film layers N, temperature T, and the two parameters α and W_0/V_0 of the model. Having obtained the set of OPs q_i and $\sigma_i(i=1,\ldots,N)$, one can calculate the dimensionless Helmholtz free energy per molecule for each layer as

$$f_1=\frac{1}{6}\left[\frac{W_0}{V_0}q_1\left(\frac{W_0}{V_0}q_1+q_2\right)+\alpha\frac{W_0}{V_0}\sigma_1\left(\frac{W_0}{V_0}\sigma_1+\sigma_2\right)-2\theta\ln Q_1\right],$$

$$f_{1<i<N}=\frac{1}{6}\left[q_i\sum_{j=i-1}^{i+1}q_j+\alpha\sigma_i\sum_{j=i-1}^{i+1}\sigma_j-2\theta\ln Q_i\right],$$

$$f_N=\frac{1}{6}\left[\frac{W_0}{V_0}q_N\left(\frac{W_0}{V_0}q_N+q_{N-1}\right)+\alpha\frac{W_0}{V_0}\sigma_N\left(\frac{W_0}{V_0}\sigma_N+\sigma_{N-1}\right)-2\theta\ln Q_N\right],\tag{5}$$

where $\theta=\frac{3k_BT}{V_0}$ is the dimensionless temperature, $f_i=\frac{F_i}{N_iV_0}$ is the dimensionless Helmholtz free energy corresponding to the ith layer, $f=\frac{1}{N}\Sigma_{i=1}^{N}f_i$ is the full dimensionless Helmholtz free energy per molecule, and $Q_i=\frac{1}{d}\int_{(i-1)d}^{id}dz\int_0^1h_i(x,z)dx$, $(i=1,\ldots,N)$ is the partition function of the ith layer, respectively. Since our purpose is also to account for the experimentally observed phenomenon of the stepwise reduction of the value of heat capacity as the temperature is raised above the bulk smectic A-isotropic transition temperature θ_{AI}(bulk) [2], one must first calculate the entropy of the system per molecule $s=\frac{1}{N}\Sigma_{i=1}^{N}s_i$, where

$$-\frac{\theta}{3}s_i = 2f_i + \frac{\theta}{3}\ln Q_i, (1 \le i \le N). \quad (6)$$

Here $s_i = \frac{S_i}{N_i k_B}$ is the dimensionless entropy per molecule corresponding to the ith layer. Finally, the dimensionless heat capacity of the smectic film per molecule at constant volume $v = V/M$ is given by [15,19]

$$c_v = \frac{C_v}{Mk_B} = \frac{T}{Mk_B}\left(\frac{\partial S}{\partial T}\right)_v = \theta\left(\frac{\partial s}{\partial \theta}\right)_v. \quad (7)$$

It should be pointed out that a number of calorimetric measurements of the heat capacity have been carried out at constant pressure [2,18] $c_p = \frac{T}{Mk_B}(\frac{\partial S}{\partial T})_P = \theta(\frac{\partial s}{\partial \theta})_P$, but in our case of free-standing smectic films [19] $c_p - c_v = \frac{Tv\alpha^2}{\kappa_T} = 0$, because $\frac{\partial v}{\partial T}$ is equal to 0. Here $\alpha = \frac{1}{v}(\frac{\partial v}{\partial T})_P$ is the volume expansion coefficient, whereas $\kappa_T = -\frac{1}{v}(\frac{\partial v}{\partial P})_T$ is the isothermal compressibility of the FSSFs.

Equations (1)–(7) are the relations which are needed to calculate both the structural and thermodynamic properties of the free-standing smectic films. Here we choose the set of parameters N, α, and W_0/V_0 corresponding to the partially fluorinated HmFnMOPP [2] compound, where m and n give the number of carbons in the hydrocarbon and fluorocarbon tails, respectively. Taking into account that both calorimetric and optical reflectivity studies on free-standing partially fluorinated 5-n-alkyl-2-(4-n-(perfluoroalkyl-metheleneoxy)phenyl) (H10F5MOPP) films were carried out with initially 25-layer thick films above the bulk SmA-Isotropic transition temperature [T_{AI}(bulk) ~ 358 K], we choose, first of all, that the initial film thickness is equal to $N=25$. According to the McMillan theory [15] a first-order bulk AI transition occurs for $\alpha \ge 0.98$, so, our choosing of $\alpha = 1.05$ is acceptable and in agreement with previous calculations of the physical properties of FSSFs [14,20,21]. As for the value of W_0/V_0, one can be guided by the fact that the FSSFs studied are stable above the bulk SmA-Isotropic transition temperature. This allows us to assume that the value of the interaction constant W_0 should be greater than V_0. So, first of all, in further calculations we will study the cases of strong surface-enhanced pair interactions with $W_0 = 5V_0$ and $10V_0$. Taking into account that the partially fluorinated compound H10F5MOPP has bulk SmA-I transition temperature T_{AI}(bulk) ~ 358 K, [θ_{AI}(bulk) ~ 0.675] and for $\alpha = 1.05$, according to the McMillan theory [15], the value of $k_B T_{AI}$(bulk)$/0.2202V_0 = 1.021$, one can estimate that the value of V_0 is equal to $\sim 2.2 \times 10^{-20}$ J. In our calculations, the dimensionless temperature $\theta = \frac{3k_B T}{V_0}$ varies between 0.60 (~318.2 K) and 0.80 (~424.3 K).

The temperature θ's effect both on the orientational $q_i(\theta)$ and translational $\sigma_i(\theta)$ OPs in the smectic film with $N=25$ layers has been investigated numerically by solving the set of $2N$ self-consistent nonlinear Eqs. (2)–(4) and is shown in Figs. 1(a) and 1(b). The model parameters used in these calculations are $N=25$, $\alpha = 1.05$, and $W_0 = 5V_0$. In the low-temperature region $0.60 \le \theta \le 0.675$(318.2 K $\le T \le$ 358 K), these equations have a stable unique solution, which is characterized by high values of the corresponding orientational

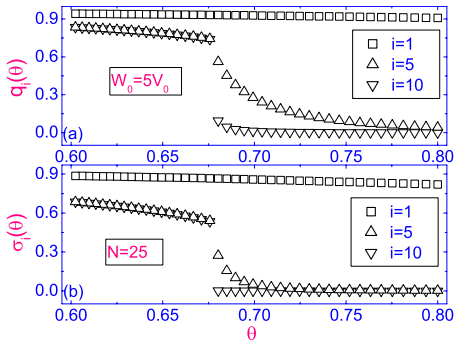

FIG. 1. (Color online) Orientational $q_i(\theta)$ ($i=1,5,10$) (a) and translational $\sigma_i(\theta)$ ($i=1,5,10$) (b) OPs as the function of dimensionless temperature θ. Here the set of model parameters are $N=25$, $\alpha=1.05$, and $W_0=5V_0$, whereas $i=1,5,10$ are the layer numbers in the smectic film with initially $N=25$ layers.

$q_i(\theta)$ [Fig. 1(a), squares and up and down triangles] and translational $\sigma_i(\theta)$ OPs [Fig. 1(b), squares and up and down triangles], both in the vicinity of the bounding surfaces, as well as near the film center. In the high-temperature region $0.685 \le \theta \le 0.8$(363.3 K $\le T \le$ 424.3 K), one also has a stable unique solution, which is characterized by vanishing of both OPs $q_i(\theta)$ and $\sigma_i(\theta)$ near the film center, whereas in the vicinity of the bounding surfaces, both OPs still maintain relatively high values. In Ref. [14], this type of solution was called a "quasi-smectic" state. At intermediate temperatures $0.675 \le \theta \le 0.685$(358 K $\le T \le$ 363.3 K), both types of solutions of the self-consistent equations exist, although for clarity Fig. 1 shows only the quasismectic profiles. In these cases, the profiles demonstrate strong ordering in the vicinity of the bounding surfaces, due to the stronger pair interactions within the first and last layers than for all interior layers, which decreases rapidly with distance from those surfaces. Note that both the orientational $q_i(\theta)$ [Fig. 1(a), up triangles ($i=5$)] and translational $\sigma_i(\theta)$ [Fig. 1(b), up triangles ($i=5$)] OPs fall continuously to some finite values, whereas those parameters corresponding to the interior layers close to the film center [Figs. 1(a) and 1(b), down triangles ($i=10$)] drop to 0.

As described later, based on the behavior of the free energy, we calculate that the layer-thinning transition temperature for the case of $N=25$ layers occurs at $\theta_{AI}(N=25) \sim 0.678$[$T_{AI}(N=25) \sim 359.6$ K]. Here $\theta_{AI}(N=25)$ and $T_{AI}(N=25)$ denote the dimensionless and dimensional layer-thinning transition temperatures, respectively, in the case of strong ($W_0=5V_0$) "enhanced" pair interactions in the bounding layers.

According to our calculations, the distributions of the OPs $q_i(\theta)$ and $\sigma_i(\theta)$ across the 25 layer smectic film, at three dimensionless temperatures $\theta=0.65$(~344.74 K), 0.67 (~355.35 K), and 0.69 (~366 K), are characterized by a monotonic decrease of both $q_i(\theta)$ and $\sigma_i(\theta)$ with increasing distance (or number of layers) from the bounding surface toward the interior of the film. In the case of strong ($W_0=5V_0$) "enhanced" pair interactions in the bounding layers, [see Figs. 2(a)–2(c)] these distributions are characterized by minima in the middle part of the film and decreasing values of these OPs with increase in temperature.

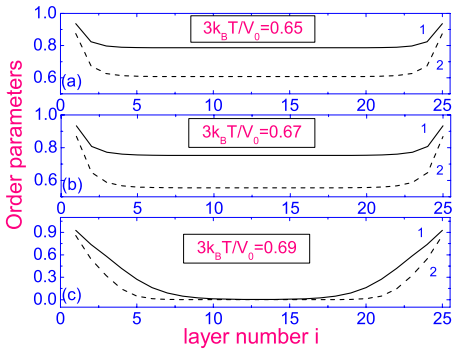

FIG. 2. (Color online) Orientational q_i (curves 1) and translational σ_i (curves 2) OPs as functions of layer number i for different temperatures; (a) θ=0.65, (b) 0.67, and (c) 0.69, respectively. Here the set of model parameters is the same as in Fig. 1.

Having obtained the profiles of OPs q_i and σ_i for different values of the temperature, one can calculate, by using Eqs. (5) and (6), the distributions both of the dimensionless Helmholtz free energy $f(i)$ [Fig. 3(a)] and entropy $s(i)$ [Fig. 3(b)]. This was done for a number of temperatures: θ=0.66 (down triangles), 0.665 (up triangles), and 0.67 (squares), respectively. In these cases, the free-energy profiles demonstrate monotonic growth of the value of $f(i)$ up to the eighth layer from each boundary, where the function $f(i)$ saturates and does not change with further increase of i. Physically, this means that all film layers are subjected to attractive forces from the bounding surfaces. Note that at temperatures close to the layer-thinning value $\theta_{AI}(N=25)\sim 0.678$, strong ordering takes place only in the vicinity of the bounding surfaces, whereas far from the surfaces ordering drops to lower values than in the bounding layers, as shown earlier in Fig. 1. As a result, we find that when the temperature varies from below $\theta_{AI}(N=25)$ to a lower value θ=0.66, there are smaller differences between the Helmholtz free energy $f(i)$ profiles, see Fig. 3(a), contrasting the up and down triangles from the squares. The same tendency can be seen in the case of the entropy $s(i)$ profiles [see Fig. 3(b)].

With increasing temperature, one finds a dramatic change of the free-energy profiles. When the layer-thinning transition temperature corresponding to the case of strong interaction with $W_0=5V_0\{\theta_{AI}(N=25)\sim 0.678[T_{AI}(N=25)\sim 359.6$ K]} for a film initially containing 25 layers is reached, the interior layers become unstable and the system undergoes the discontinuous transition to the quasismectic state [14], an effect seen earlier in the behavior of the order parameters in Fig. 1. The distributions of both the free energy and entropy in the high-temperature region $\theta>0.678$ are shown in Figs. 4(a) and 4(b), for temperatures θ=0.68 (squares), 0.685 (up triangles), and 0.69 (down triangles), respectively. Now the distribution of the free energy over the film layers is characterized by maxima in the vicinity of both bounding surfaces. It allows us to conclude that the forces acting on the interior layers are in the opposite direction to the attractive ones. As a result, the interior layers are squeezed by the bounding layers.

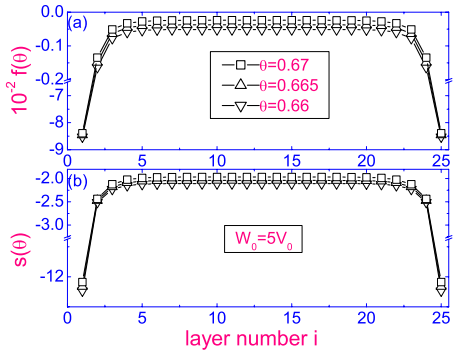

FIG. 3. (Color online) Dimensionless Helmholtz free energy $f(i)$ (a) and entropy $s(i)$ (b) as functions of layer number i, for three dimensionless temperatures θ=0.66 (down triangles), 0.665 (up triangles), and 0.67 (squares), respectively. The set of model parameters is the same as in Fig. 1.

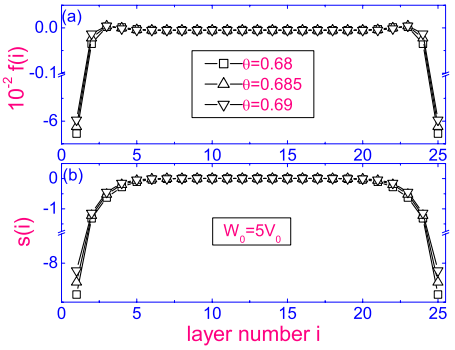

FIG. 4. (Color online) Same as in Figs. 3(a) and 3(b), but the temperatures are θ=0.68 (squares), θ=0.685 (up triangles), and 0.69 (down triangles), respectively.

Because we are primarily focusing both on describing the heat capacity in the vicinity of the layer-thinning transition temperatures corresponding to the case of strong surface interactions and, in particular, the stepwise reduction of the value of $c_v(N)$ as the temperature is raised above the bulk smectic A-isotropic transition, the temperature θ's effect on the dimensionless Helmholtz free energy $f(\theta)$ and entropy $s(\theta)$ of a smectic film at constant volume are shown in Figs. 5(a), 5(b), 6(a), and 6(b). The model parameters used in the calculations are α=1.05 and $W_0=5V_0$, for a number of film thicknesses; N=25 (curve 1), N=13 (curve 2), and N=11 (curve 3) [Figs. 5(a) and 5(b)], and N=10 (curve 1), N=8 (curve 2), and N=6 (curve 3) [Figs. 6(a) and 6(b)], respectively. Our calculations show that the SmA-I transition occurs through a sequence of layer-thinning transitions $25\rightarrow 13\rightarrow 11\rightarrow 10\ldots$, as the temperature is increased. The calculated Helmholtz free energy per molecule for the 25-layer thick film is shown in Fig. 5(a) (curve 1) vs dimensionless temperature θ, and demonstrates smooth behavior with increase of θ, whereas the value of $s(\theta)$ [Fig. 5(b), (curve 1)] demonstrates a discontinuous rise at $\theta_{AI}(N=25)\sim 0.678[T_{AI}(N=25)\sim 359.6$ K] greater than $40k_B$ per molecule, due to the transition to the quasismectic state and corresponding change in slope of the free-energy curves. A similar discontinuity in $s(\theta)$ is seen in Fig. 6(b) for N=10 (curve 1). Discontinuities in $s(\theta)$ occur for the other values of N, but are not seen in the figures due to the fixed vertical length scale.

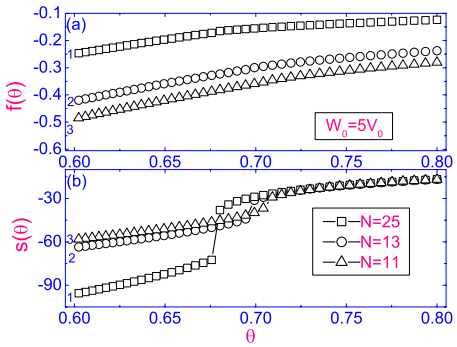

FIG. 5. (Color online) (a) Dimensionless Helmholtz free energy $f(\theta)$ as a function of dimensionless temperature θ, corresponding to three film thicknesses: $N=25$ (curve 1), 13 (curve 2), and 11 (curve 3), respectively. Here the set of model parameters are the same as in Fig. 1(b) Same as (a), but for the dimensionless entropy $s(\theta)$.

Following the transition of an N-layer film to the quasismectic state, we determine the number of layers $(N-n)$ remaining in the film with nonvanishing smectic order near the film center to be such as to provide a lower free energy than the N-layer state at the same temperature as well as having a higher transition temperature. Based on this mechanism, our calculations show that the next stable state with lower free energy occurs at $N=13$, then at $N=11$, etc. The corresponding layer-thinning temperatures $\theta_{\mathrm{AI}}(N)$ are: $\theta_{\mathrm{AI}}(N=25) \sim 0.678(\sim 359.6\ \mathrm{K})$, $\theta_{\mathrm{AI}}(N=13) \sim 0.697(\sim 369.7\ \mathrm{K})$, $\theta_{\mathrm{AI}}(N=11) \sim 0.706(\sim 374.44\ \mathrm{K})$, $\theta_{\mathrm{AI}}(N=10) \sim 0.7106(\sim 377\ \mathrm{K})$, $\theta_{\mathrm{AI}}(N=9) \sim 0.717(\sim 380.3\ \mathrm{K})$, $\theta_{\mathrm{AI}}(N=8) \sim 0.729(\sim 386.6\ \mathrm{K})$, $\theta_{\mathrm{AI}}(N=7) \sim 0.736(\sim 390.3\ \mathrm{K})$, $\theta_{\mathrm{AI}}(N=6) \sim 0.743(\sim 394\ \mathrm{K})$, etc.

It should be pointed out here that our determination of layer-thinning transition temperatures (given above) does not follow the method described by Mirantsev [14], which is based on the location of the upper spinodal limits of overheated smectic films. Rather our approach is equivalent to that discussed in Ref. [20], where the smectic to quasismectic transition occurs when both phases have equal free energy. For example, the layer-thinning transition temperature for $N=25$ in [14] was calculated to equal $\bar{\theta}_{AI}(N=25) \sim 0.69[T_{AI}(N=25) \sim 366\ \mathrm{K}]$, at which the set of self-consistent Eqs. (2) and (3) loose the solution with nonvanishing smectic order in the central layers of the N-layer film.

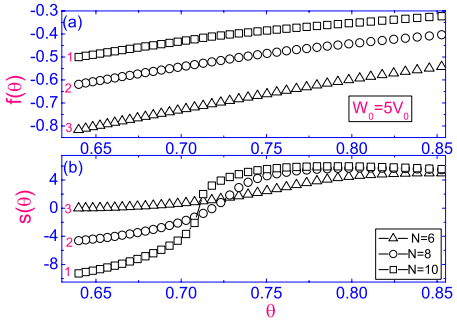

FIG. 6. (Color online) (a) and (b). Same as in Figs. 5(a) and 5(b), but the film thicknesses are: $N=10$ (curves 1), 8 (curves 2), and 6 (curves 3), respectively.

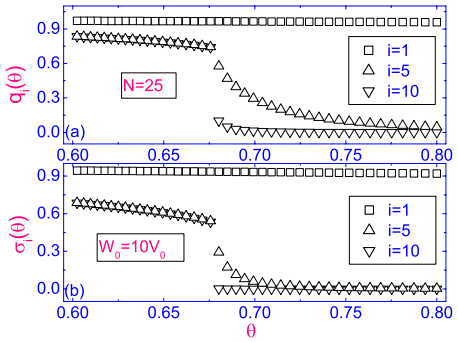

FIG. 7. (Color online) Same as in Figs. 1(a) and 1(b), but in the case of strong interaction $W_0=10V_0$.

This value is well above the value $\theta_{AI}(N=25) \sim 0.678$ reported here, and shows that in the intermediate temperature range, both kinds of solution are locally stable.

With increase in the value of W_0 by two times, from $5V_0$ to $10V_0$, the self-consistent equations also have locally stable solutions which are characterized by higher values of the orientational $q_i(\theta)$ [Fig. 7(a)] and translational $\sigma_i(\theta)$ OPs [Fig. 7(b)] (squares) near the bounding surfaces, than close to the film center [see Figs. 7(a) and 7(b)], both up and down triangles, respectively). In that case, as in the case of weaker surface interaction $W_0=5V_0$, both the nematic and smectic OPs are coupled together and drop discontinuously to 0 near the layer-thinning transition temperature $\bar{\theta}_{AI}(N=25) \sim 0.678[T_{AI}(N=25) \sim 359.6\ \mathrm{K}]$. The calculated dimensionless Helmholtz free energy, entropy, and heat capacity per particle vs temperature, in the case of $W_0=10V_0$ (not shown), demonstrate the same qualitative behavior as in the case of weaker interactions with $W_0=5V_0$.

The temperature θ's effect on the dimensionless heat capacity at constant volume $c_v(\theta)$ of a smectic film with 25 layers, in the two cases of strong interactions $W_0=5V_0$ and $10V_0$ is shown in Figs. 8(a) and 8(b), respectively.

It is clear that the heat capacity $c_v(\theta) \sim 10^4$ anomaly (i.e., heat-capacity peaks) [Fig. 8(a)] at temperature $\theta_{AI}(N=25) \sim 0.678[T_{AI}(N=25) \sim 359.6\ \mathrm{K}]$, is associated with the interior first-order SmA-I transition, where the entropy change is greater than $40k_B$ [Fig. 5(b), curve 1] per molecule, and demonstrates a discontinuous rise at $\theta_{AI}(N=25)$, whereas the

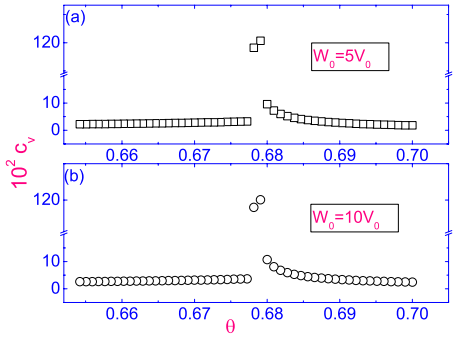

FIG. 8. (Color online) (a) Dimensionless heat capacity $c_v(\theta)$ as a function of dimensionless temperature θ. Here the set of model parameters are $N=25$, $\alpha=1.05$, and $W_0=5V_0$. (b) Same as (a), but the interaction constant W_0 is equal to $10V_0$.

TABLE I. The calculated, using Eqs. (1)–(7), and measured (by means of calorimetric techniques [2]) data on the heat capacity in free-standing partially fluorinated H10F5MOPP smectic films.

	(Temp.)	(Theor.)	(Theor.)		(Temp.)	(Expt.)
N (Theor.)	$\theta(N)$ (Theor.)	$c_v(N)$	$C_v(N)[\frac{\mu J}{cm^2\,K}]$	N (Expt.)	$\theta(N)$ (Expt.)	$C_p(N)[\frac{\mu J}{cm^2\,K}]$
25	0.674	420	82.5	25	0.674	80
13	0.685	264	52	15	0.676	48
11	0.702	215	42.4	11	0.678	35
10	0.708	184	36.3	9	0.68	30
9	0.711	155	31	8	0.682	25
8	0.722	134	27	7	0.684	22
7	0.73	117	23	6	0.686	18
6	0.741	85	17			

value of $c_v(\theta)$ [Fig. 8(a)], in the temperature range $0.655 \leq \theta \leq 0.677$, varies between 280, at $\theta \sim 0.655$, and 450, at $\theta = 0.677$, respectively. Note that in the case when the "enhanced" pair interactions in the bounding layers have $W_0 = 10V_0$, two times stronger than the abovementioned case, the calculated dimensionless heat capacity per molecule vs temperature demonstrates the same qualitative behavior [see Fig. 8(b)] and the value of the layer-thinning transition temperature $\bar{\theta}_{AI}(N=25)$ is practically the same as in the weaker case [see Figs. 7(a) and 7(b)]. In the temperature range $0.655 \leq \theta \leq 0.677$, the value of $c_v(\theta)$ [Fig. 8(b)] varies between 300, at $\theta \sim 0.655$, and 480, at $\theta = 0.677$, respectively.

In order to make direct comparison between calculated and measured (by means of calorimetric techniques [2]) data on the heat capacity of a partially fluorinated H10F5MOPP 25-layer film, the $c_v(\theta) \sim 420$, or ~ 82.5 $[\frac{\mu J}{K\,cm^2}]$, or $\sim 5.74 \times 10^{-21}$ $[\frac{J}{K\,mol}]$ was calculated at temperature $\theta \sim 0.674$ (~ 357 K), below both the bulk SmA-Isotropic transition temperature and the layer-thinning transition temperature corresponding to strong ($W_0 = 5V_0$) interactions in the bounding layers. The measured value of C_P, at the same temperature corresponding to "plateau" values of the heat capacity, is equal to ~ 80 $[\frac{\mu J}{cm^2\,K}]$, or $\sim 5.9 \times 10^{-21}$ $[\frac{J}{K\,mol}]$. Hence, we obtain good agreement between the theoretically predicted and experimentally obtained results. In recalculations of the theoretical values of $c_v(N)$ per H10F5MOPP molecule in order to compare with the measured $C_p(N)$ values, we use the fact that the total number of molecules M per unit area in the film, denoted n_s, can be estimated as $n_s = n_0 l$, where $n_0 \sim 1.5 \times 10^{21}$ cm^{-3} is the number density and $l = Nd$ is the thickness of the N-layer film. Since d is of the order of the molecular length ~ 3.0 nm [22], n_s can be estimated as $n_s \sim N \times 4.5 \times 10^{14}$ cm^{-2}.

Based on these results, we conclude that the extended Mc Millan's approach "enhanced" by anisotropic interactions in the bounding layers, with $W_0 = 5V_0$, is more suitable for describing both the structural and thermodynamic properties of a partially fluorinated H10F5MOPP smectic film, than with $W_0 = 10V_0$, which gives $c_v \sim 450$, or ~ 86.7 $[\frac{\mu J}{K\,cm^2}]$, at temperature $\theta \sim 0.674 (\sim 357$ K).

Collected in Table I are the calculated data on the dimensionless heat capacity $c_v(N)$ per molecule, and the recalculated dimensional heat capacity $C_v(N)$, corresponding to N layer films, as well as the "plateau" temperatures $\theta(N)$ for the sequence of the abovementioned layer-thinning transitions (with $W_0 = 5V_0$). These plateau temperatures satisfy: $\theta(25) < 0.678 < \theta(13) < 0.697 < \theta(11) < 0.706 < \theta(10) < 0.7106 < \theta(9) < 0.717 < \theta(8) < 0.729 < \theta(7) < 0.736 < \theta(6) < 0.743$, where the numbers correspond to the successive layer-thinning transition temperatures given earlier. The observed data on $C_p(N)$ for the free-standing partially fluorinated H10F5MOPP smectic films also correspond to a series of "plateau" values for the sequence of the layer-thinning transitions $25 \rightarrow 15 \rightarrow 11 \rightarrow 9 \rightarrow 8 \ldots$ etc. [2]. In the range of film thicknesses investigated, the reduction of $C_v(N)$ is, at least qualitatively, in agreement with the experimentally observed decrease of $C_p(N)$ with decrease of N.

III. CONCLUDING REMARKS

These results indicate that the relatively simple mean-field approach, based on the extended McMillan theory, can be usefully applied for describing both the structural and thermodynamic properties of free-standing smectic films. By solving the self-consistent nonlinear equations for the order parameters, at least for two clearly distinct regimes of strong surface interactions with $W_0 = 5V_0$ and $10V_0$, we observed both the heat-capacity anomalies and the stepwise reduction of the value of $c_v(N)$ at temperatures above the bulk transition, with the surface layers being more ordered than the internal ones. With enhanced pair interactions in the bounding layers, the smectic-isotropic transition corresponds to smectic melting of the central layers. This is in accord with the well established scenario of melting in such quasi-two-dimensional systems, where the melting originates in the interior of the smectic film and penetrates toward the surface.

Our calculations with $N = 25$, $\alpha = 1.05$, $\theta_{AI}(N=25) = 0.678$, and $W_0 = 5V_0$ show that the present and previous calculations with $W_0 = 3V_0$ in the framework of Mirantsev's model [14] (not shown in the text), give close agreement for the order parameters, whereas the values of the Helmholtz free energy, entropy, and heat capacity have different values, due to differences in the expressions for these thermodynamic functions (see Eqs. (5)–(7) and Eqs. (12)–(14) of Ref. [14]).

Slight differences between the theoretical and experimental plateau temperatures in Table I are most likely due to the fact that the present model is still very primitive for a proper description of many delicate processes in partially fluorinated compounds. Only one of the parameters of the model (α, related to the length of the alkyl tails) has been fitted to the real behavior of the LC molecules.

It should be noted that there is not yet a clear consensus on the mechanisms by which layer-thinning occurs. According to the set of mean-field theories followed here [10,14,23,24], thinning takes place when the smectic layer structure throughout the middle of the film vanishes. In an alternative theory [25], supported by experimental study [26,27], layer-thinning occurs in compounds which undergo first-order SmA-I transitions by spontaneous nucleation of dislocation loops, the growth of which causes a film to thin. A model of this process was described in Ref. [25], predicting a layer-thinning transition temperature $T_{AI}(N)$ dependence which is functionally different from the power-law relation first described in [2] but which fits experimental data closely. Another mean-field theory, based on the generalization of the de Gennes model for a "presmectic" fluid confined between two solid walls by means of including a quadratic term in the surface smectic OP while neglecting the external field term, also presents a simple analytical formula for variation of $T_{AI}(N)$ with N which also fits experimental data very closely [16]. Hence, further study on a wider range of compounds will be required to sort through the correlation between the transition temperatures resulting from the mean-field approaches and experimental measurements. In particular, it would be worthwhile to perform studies on series of compounds that extends the range of the parameter α. Recall that α, according to McMillan's model, can vary from 0 to 2. For instance, for $\alpha < 0.98$, McMillan's model predicts an intermediate nematic phase. Hence, it would be worthwhile to carry out similar studies on series of compounds that include the SmA-nematic phase transition, as well as in the framework of a modified version of Landau-de Gennes theory [16].

On the other hand, comparisons of the theoretical and experimental stepwise reductions of heat-capacity values at "plateau" regions in homogeneous films away from the layer-thinning transition temperatures, as carried out in this work, should be unaffected by questions of the layer-thinning mechanisms. Nonetheless, these mechanisms may affect the "anomalies" shown by the heat-capacity peaks in Fig. 8. Such anomalies have not been presented in experimental studies of SmA layer-thinning transitions, to our knowledge, but only in studies of SmA to hexatic-B transitions of free-standing films [9], and we hope the present work will spur further experimental work in this direction.

Taking into account that, from an order-of-magnitude point of view, there is good agreement between theoretical predictions and experimental results, this work lends credibility to the theoretical interpretation of the heat-capacity data and to the validity of the mean-field approach.

ACKNOWLEDGMENTS

We acknowledge financial support from NSERC (Canada). A.V.Z. acknowledges support from the Russian Funds for Fundamental Research (Grant No. 09-02-00010-a). This work was made possible by use of the facilities of the Shared Hierarchical Academic Research Computing Network (SHARCNET: www.sharcnet.ca) and Comput/Calcul Canada.

[1] W. H. de Jeu, B. I. Ostrovskii, and A. N. Shalaginov, Rev. Mod. Phys. **75**, 181 (2003).
[2] T. Stoebe, P. Mach, and C. C. Huang, Phys. Rev. Lett. **73**, 1384 (1994).
[3] D. J. Tweet, R. Holyst, B. D. Swanson, H. Stragier, and L. B. Sorensen, Phys. Rev. Lett. **65**, 2157 (1990); R. Holyst, D. J. Tweet, and L. B. Sorensen, *ibid.* **65**, 2153 (1990).
[4] R. Lucht and Ch. Bahr, Phys. Rev. Lett. **78**, 3487 (1997).
[5] A. M. Somoza, L. Mederos, and D. E. Sullivan, Phys. Rev. Lett. **72**, 3674 (1994).
[6] T. Stoebe, P. Mach, and C. C. Huang, Phys. Rev. E **49**, R3587 (1994).
[7] M. Veum, E. Kutschera, N. Voshell, S. T. Wang, S. L. Wang, H. T. Nguyen, and C. C. Huang, Phys. Rev. E **71**, 020701(R) (2005).
[8] M. Veum, M. K. Blees, N. Voshell, H. T. Nguyen, and C. C. Huang, Phys. Rev. E **74**, 011703 (2006).
[9] C. Y. Chao, C. R. Lo, P. J. Wu, T. C. Pan, M. Veum, C. C. Huang, V. Surendranath, and J. T. Ho, Phys. Rev. Lett. **88**, 085507 (2002).
[10] A. M. Somoza, L. Mederos, and D. E. Sullivan, Phys. Rev. E **52**, 5017 (1995); Y. Martinez, A. M. Somoza, L. Mederos, and D. E. Sullivan, *ibid.* **53**, 2466 (1996).
[11] E. I. Demikhov, V. K. Dolganov, and K. P. Meletov, Phys. Rev. E **52**, R1285 (1995).
[12] E. A. Mol, G. C. L. Wong, J. M. Petit, F. Rieutord, and W. H. de Jeu, Physica B **248**, 191 (1998).
[13] S. Pankratz, P. M. Johnson, H. T. Nguyen, and C. C. Huang, Phys. Rev. E **58**, R2721 (1998).
[14] L. V. Mirantsev, Phys. Lett. A **205**, 412 (1995).
[15] W. L. McMillan, Phys. Rev. A **4**, 1238 (1971).
[16] D. E. Sullivan and A. N. Shalaginov, Phys. Rev. E **70**, 011707 (2004).
[17] H. Nakanishi and M. E. Fisher, J. Chem. Phys. **78**, 3279 (1983).
[18] C. C. Huang, I. M. Jiang, A. J. Jin, T. Stoebe, R. Geer, and C. Dasgupta, Phys. Rev. E **47**, 2938 (1993).
[19] L. D. Landau and E. M. Lifshitz, *Statistical Physics*, 3rd ed., Part 2 (Butterworth-Heinemann, Oxford, 1980), Vol. 9, p. 308.
[20] A. A. Canabarro, I. N. de Oliveira, and M. L. Lyra, Phys. Rev. E **77**, 011704 (2008).
[21] M. S. S. Pereira, M. L. Lyra, and I. N. de Oliveira, Phys. Rev. Lett. **103**, 177801 (2009).
[22] P. Mach, P. M. Johnson, E. D. Wedell, F. Lintgen, and C. C.

Huang, EPL **40**, 399 (1997).
[23] E. E. Gorodetskii, E. S. Pikina, and V. E. Podnek, Zh. Eksp. Teor. Fiz. **115**, 61 (1999) [JETP **88**, 35 (1999)].
[24] A. N. Shalaginov and D. E. Sullivan, Phys. Rev. E **63**, 031704 (2001).
[25] S. Pankratz, P. M. Johnson, R. Holyst, and C. C. Huang, Phys. Rev. E **60**, R2456 (1999).
[26] J. Ch. Geminard, R. Holyst, and P. Oswald, Phys. Rev. Lett. **78**, 1924 (1997).
[27] S. Pankratz, P. M. Johnson, A. Paulson, and C. C. Huang, Phys. Rev. E **61**, 6689 (2000).